Polarization-maintaining fiber loop with double optical length and its application to fiber optic gyroscope

Changsheng Li (李长胜)*, Chunxi Zhang (张春熹), Ningfang Song (宋凝芳), and Hongjie Xu (徐宏杰)

School of Instrument Science and Optoelectronic Engineering, Beihang University, Beijing 100191, China

**Corresponding author: cli@buaa.edu.cn*

Received July 19, 2010; accepted October 28, 2010; posted online January 28, 2011

A novel polarization maintaining fiber (PMF) loop is proposed and used for an interferometric fiber optic gyroscope (FOG). By splicing a conventional PMF loop with two pigtailed polarization beam splitters, polarized light can be guided to propagate along the slow and fast axes of the PMF in sequence to double its effective optical length in the loop. In particular, the resultant optical length in the combined loop is partially self-compensated for some external disturbances, such as transverse strain. Primary experiments on the FOG using the proposed loop demonstrate that the average static bias deviation between –40 and +60 °C is less than 0.050 deg./h, and the average bias variation under conventional random vibration test is less than 0.10 deg./h.

OCIS codes: 060.2340, 060.2800, 230.5440, 350.4600.

doi: 10.3788/COL201109.020604.

Optical fiber loop has been widely used in optical sensing and communication systems, such as rotation-sensitive element in fiber optic gyroscope (FOG), optical fiber loop mirror and optical time delay line, Sagnac interferometer, and so on[1−3]. The type of optical fiber used for the loop may be single-mode fiber, polarization-maintaining fiber (PMF)[1], or hollow-core photonic crystal fiber[4]. PMF usually has two principal dielectric axes, i.e., slow and fast axes with refractive indices represented by n_s and n_f, respectively. Only a single principal axis is used in most of the previous applications; thus the optical length in the PMF loop is $n_\mathrm{s}L$ or $n_\mathrm{f}L$, where L denotes the geometric length of the PMF. Slow and fast axes have been simultaneously used in a resonant FOG to improve its bias stability using a 90° principal axis rotation in the PMF loop[5,6]. Slow and fast axes have also been simultaneously used in a frequency modulated continuous wave gyroscope to form two Sagnac interferometers[7]. However, the effective optical length for clockwise (cw) and counter-clockwise (ccw) light beam in this scheme is still $n_\mathrm{s}L$ or $n_\mathrm{f}L$. Other schemes with compact fiber loop include re-entrant interferometric FOG[8], slow-light resonator structure[9], and so on.

A small and compact optical fiber loop is ideal for many applications, such as the FOG. In this letter, we propose a novel combined PMF loop with effective optical length $(n_\mathrm{s}+n_\mathrm{f})L$. We also analyze its basic optical property and experimentally investigate its application to an interferometric FOG.

If light propagates through the slow and fast axes of the PMF in sequence, the effective optical length in the loop becomes $(n_\mathrm{s}+n_\mathrm{f})L$. To achieve this idea, one can combine a conventional PMF loop with two pigtailed polarization beam splitters (PBSs) (Fig. 1(a)). For each PBS, the slow and fast axes of its common pigtail fiber are respectively aligned with the slow axes of its two branch pigtail fibers. Here, all the fiber joints 1, 2, and 3 are spliced at 0° (Fig. 1(a)). Assuming that a linearly polarized light is launched into the pigtail fiber (21) of PBS2 along its slow axis, then through PBS2 (the slow axis of the PMF loop) and PBS1, the cw light can reach the pigtail fiber (11) of PBS1 and the pigtail fiber (22) of PBS2 to start its second turn. After propagating through PBS2, the fast axis of the PMF loop, and PBS1, the light emerges from pigtail fiber (12) to complete its cw optical path. The optical paths for cw and ccw light are shown in Fig. 1(b), in which one can see that the linearly polarized light has propagated through the slow and fast axes of the PMF loop in sequence. If we omit optical length in the two PBSs, the total effective optical length is $(n_\mathrm{s}+n_\mathrm{f})L$.

Although the difference of optical length between cw and ccw light in the above combined loop is equal to zero, the two optical paths are nonreciprocal to splicing joint 3 due to the Shupe effect which can lead to temperature-induced bias drift in the FOG[10,11]. For this, a combined PMF loop with reciprocal optical path was designed (Fig. 2 (a)). Different from Fig. 1(a), there is a fiber splicing joint 4 inside the PMF loop consisting of two segments of PMF. Joint 4 is the central point of the loop, and the fiber splicing angle is 90°. The other three joints are still spliced at 0°. The corresponding optical path is shown in Fig. 2(b). The total

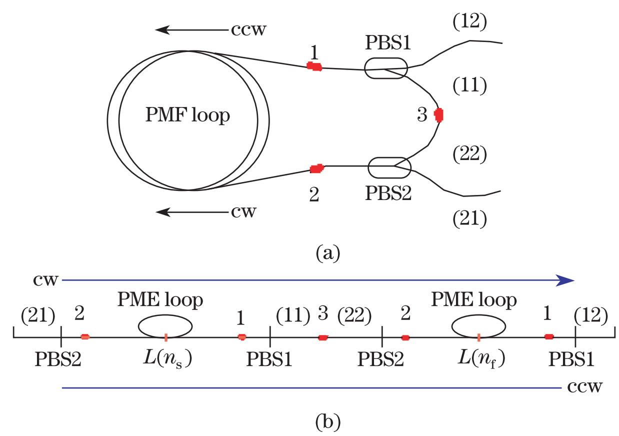

Fig. 1. (a) Configuration of the combined PMF loop with nonreciprocal optical path; (b) doubled effective optical length.

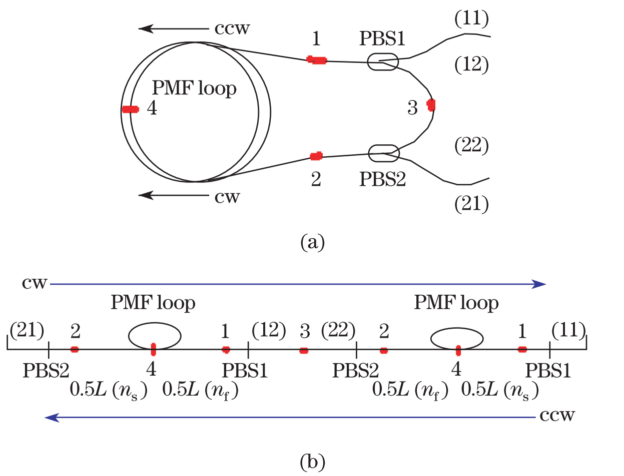

Fig. 2. (a) Configuration of the combined PMF loop with reciprocal optical path; (b) doubled effective optical length.

optical lengths for both the cw and ccw light are also $(n_\mathrm{s}+n_\mathrm{f})L$, and it is reciprocal to the central point of the whole optical path of joint 3.

The influence of strain and temperature on optical length in the above proposed loops should be considered for practical use. The Shupe effect in the conventional PMF loop has already been analyzed in the previous works[10,11]. The strain-induced change in optical length in the PMF has also been investigated. In particular, the changes in fiber length and birefringence induced by strain have been theoretically analyzed[12]. Further study on strain and temperature effects in the proposed loop should be based on the previous relevant studies. For example, as under conditions of no shear strain and neglectable length change; the changes in refractive index of slow and fast axes of fiber core due to strain and temperature are given in Ref. [13]. According to Eqs. (1) and (2) in Ref. [13], the total change in effective optical length in the above combined PMF loop can be represented as

$$(\Delta n_\mathrm{s}+\Delta n_\mathrm{f})\,L=-n_\mathrm{o}^2 L\left\{p_{12}\varepsilon_1+(p_{11}+p_{12})\frac{\varepsilon_2+\varepsilon_3}{2}-\left[\frac{2}{n_\mathrm{o}^3}\frac{\mathrm{d}n_0}{\mathrm{d}T}+(p_{11}+2p_{12})\sigma\right]\Delta T\right\},\quad(1)$$

where n_0 is the average refractive index of the fiber core; ε_1 is the longitudinal strain along fiber axis; ε_2 and ε_3 are two transverse strains, respectively; σ is the thermal expansion coefficient; p_{11} and p_{12} are the Pockels constants of the fiber core; ΔT is the temperature change. Equation (1) shows that the change in effective optical length is independent of transverse strain difference $(\varepsilon_2-\varepsilon_3)$.

According to the above optical designs (Figs. 1 and 2), two types of combined loops have been fabricated using two PMF loops and two PBSs with pigtail fibers. There are two approaches utilized in measuring effective optical length in the PMF loops, one is based on the measurement of transit time of light traveling forward through the fiber loop, τ, and another approach is to use optical time domain reflector (OTDR) based on the measurement of the delay time of the backward light reflected from the loop. If τ is given, we can calculate the effective geometric length of the loop, L', using the formula,

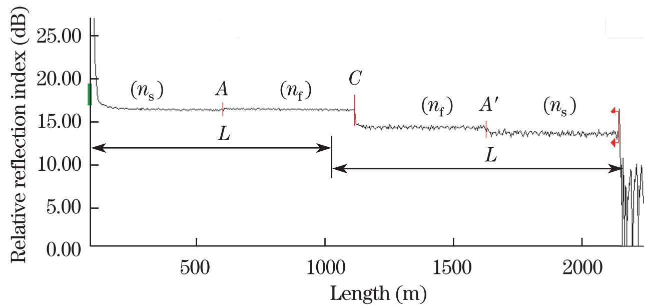

Fig. 3. Reflection index trace for the combined loop shown in Fig. 2(a) recorded using OTDR.

$L'=\tau c/n$. Here, a fiber loop is wrapped using a segment of Panda-style PMF with $L=515$ m. The first combined loop was fabricated by splicing this PMF loop with two pigtailed PBSs (Fig. 1(a)). The transit time was measured ($\tau=5.223$ μs). Provided that the speed of light in free space is $c=2.9979\times10^8$ m/s and the refractive index of the PMF core is $n=1.5$, the effective length calculated according to the above formula is $L'=1044$ m $\approx 2L$. In addition, we also measured the effective length using the OTDR, the result was $L'=1050$ m $\approx 2L$.

To fabricate the second combined PMF loop (Fig. 2(a)), two coils of identical PMFs with the same length of 510 m were simply spliced at 90°, thus the total geometric length of the loop was $L=1020$ m. There was no glue in this loop. After splicing the loop with two pigtailed PBSs according to Fig. 2(a), we measured the effective length of the combined loop using the OTDR, resulting in $L'=2049.6$ m $\approx 2L$. Figure 3 shows the OTDR-recorded reflection index trace for the second combined loop, where points A and A' correspond to the fiber splicing joint 4, which is the center of the original loop, and point C corresponds to the splicing joint 3, which is the center of the optical path in the combined loop. Given that joint 3 is outside of the original loop, we arrive at a simple approach to adjust the central position of the combined loop to maintain its symmetry. This feature is useful for its application to the FOG.

The first combined loop shown in Fig. 1(a) has been used in a closed-loop interferometric FOG. At room temperature, the gyroscope output was proportional to the rotation speed to be measured in the range of ±(1–50) deg./s. The corresponding nonlinearity of speed scale factor was less than 3.5×10^{-5}. This primary experiment demonstrates that the first combined loop is applicable for the interferometric FOG. The static bias of the FOG versus temperature has been tested in the temperature range from –40 to +60 °C. The average static bias within 2 h was –9.462 deg./h at –40 °C, and –9.412 deg./h at +60 °C, so that the static bias deviation at the two typical temperature points was 0.050 deg./h (Table 1). For comparison, the experiment on temperature characteristic of the FOG using the original PMF loop was also carried out. The results are listed in Table 1, which shows that the static bias deviation has been reduced using the combined loop. However, the static bias drift is about ±5 deg./h when the temperature varies at a rate of ±1 °C/min. This large bias drift is probably caused by the nonreciprocal optical path and the Shupe effect in the first combined loop.

Table 1. Respective Experimental Data of Temperature and Vibration Characteristics of the FOGs Using a PMF Loop and a Combined PMF Loop with Two PBSs

Experimental Conditions	Average Static Bias Versus Temperature (deg./h)			Average Bias Variation under Random Vibration (deg./h)		
	−40 °C	+60 °C	Deviation	X-Axis	Y-Axis	Z-Axis
Conventional PMF Loop	8.083	8.472	0.389	0.25	0.03	0.51
Combined PMF Loop	−9.462	−9.412	0.050	0.10	0.10	0.04

The second combined PMF loop was fabricated only for the effective optical length measurement. At present, this loop has not been used for FOG-related experiments because it is not yet a usable loop with glue. However, it is expected that the Shupe effect in this loop can be greatly suppressed due to its reciprocal optical path.

The conventional random vibration test for the above FOG was also carried out at room temperature. The average bias variations under random vibration for three orthogonal axes of the original loop are listed in Table 1. The average bias variations for the three axes are less than 0.10 deg./h within the frequency range of 20−2000 Hz. The bias variations of the FOG using conventional PMF loop under random vibration was also measured. The corresponding experimental data are also listed in Table 1. We can see that the average bias variations of the FOG using the above combined loop has been cut down for the X- and Z-axis.

According to the above optical design and experiments, and compared with the primary PMF loop, the combined PMF loop with PBS has three main features. Firstly the effective optical length is doubled. At the cost of additional two PBSs and their optical losses, the proposed loop is fiber-saving, especially for a PMF loop with a longer length, such as 1 km. In addition, compared with the conventional PMF loops, the application of PBS in the combined loop can reduce polarization noise. However, polarization cross-talk can still occur between two orthogonal eigen-modes in the PMF if any fiber splicing angle is not exactly equal to 0° or 90°. Secondly, different from the conventional PMF loop, the effective optical length in the combined loop is not $n_f L$ or $n_s L$ but $(n_f+n_s)L$. Thus, any opposite change in n_f and n_s caused by external disturbance can be suppressed or compensated with each other, e.g., transverse strain. In addition, from Eq. (1), the resultant optical length change caused by strains can also be suppressed by synchronous temperature fluctuation. Thirdly, for the combined loop in Fig. 2, the central point of the effective optical path is outside the primary PMF loop, and this feature is beneficial to the FOG. Although the optical path in the combined loop shown in Fig. 1 is nonreciprocal, it can be used for optical delay line or the FOG based on frequency modulated continuous wave[7].

Apart from different configurations, the usage of slow and fast axes in the combined PMF loop is also different from the usage in Ref. [7]. In Ref. [7] Zheng simultaneously used the slow and fast axes of the PMF to form two Sagnac interferometers, but the optical length in each interferometer was still $n_f L$ or $n_s L$ and had no mutual compensation property. In addition, there were two lightwave beams propagating along the PMF. The proposed loops mentioned above use the slow and fast axes of the PMF in sequence, the effective optical length is $(n_f+n_s)L$ with self-compensation property, and there are four lightwave beams propagating along the PMF. Compared with the previous re-entrant interferometric FOG[5,6] and resonant FOG[8], apart from the above-mentioned features, the FOG with combined PMF loop has simpler signal processing circuit and can use low-coherent or superluminescent diode as light source, however, the resonant FOG must use high-coherent laser source.

Further investigations on the proposed loop and its application to the FOG may include optical spectrum characteristic and four-wave mutual interaction inside the loop, the Shupe effect for its application to the FOG, and experiments on the second combined PMF loop in Fig. 2 for the FOG, ect.

In conclusion, a novel combined PMF loop has been designed and used for an interferometric FOG. The advantages of the proposed loop mainly include double effective optical length and its self-compensation property for some external disturbances, such as transverse strain and improved temperature and vibration stability, compared with the conventional PMF loops. Obvious disadvantages mainly include the cost of two additional PBSs and their extra optical loss. There are still some unknown and meaningful features to be further investigated for the proposed loop.

The authors would like to thank Dr. Xi Zhang for the assistance she provided in our experiments.

References

1. B. Culshaw, Meas. Sci. Technol. **17,** R1 (2006).
2. O. Frazao, J. M. Baptista, and J. L. Santos, Sensors **7,** 2970 (2007).
3. W. Chen, Y. Xie, P. Zhang, and L. Lin, Chin. Opt. Lett. **7,** 186 (2009).
4. S. W. Lloyd, V. Dangui, M. J. F. Digonnet, S. Fan, and G. S. Kino, Opt. Lett. **35,** 121 (2010).
5. L. K. Strandjord and G. A. Sanders, Proc. SPIE **1585,** 163 (1991).
6. K. Takiguchi and K. Hotate, IEEE Photon. Technol. Lett. **3,** 88 (1991).
7. J. Zheng, IEEE Photon. Technol. Lett. **17,** 1498 (2005).
8. D. N. Chen, K. Motoshima, M. M. Downs, and E. Desurvire, IEEE Photon. Technol. Lett. **4,** 813 (1992).
9. J. Scheuer, Opt. Lett. **34,** 1630 (2009).
10. D. M. Shupe, Appl. Opt. **19,** 654 (1980).
11. F. Mohr, J. Lightwave Technol. **14,** 27 (1996).
12. Y. Liao, *Fiber Optics* (Tsinghua University Press, Beijing, 2000) pp.186-191.
13. R. H. Chu and J. J. Zou, Opt. Fiber Technol. **16,** 151 (2010).